Three Ca^{2+} channel inhibitors in combination limit chronic secondary degeneration following neurotrauma

*Donna L. Savigni [a,b], *Ryan L. O'Hare Doig [a,b], Charis R. Szymanski [a,b], Carole A. Bartlett [a,b], Ivan Lozić [a,c], Nicole M. Smith [a,c], Melinda Fitzgerald [a,b].

* equal contribution.

[a]Experimental and Regenerative Neurosciences, [b]School of Animal Biology, [c]School of Chemistry and Biochemistry, The University of Western Australia, Crawley, 6009, WA, Australia.

Corresponding Author: Melinda Fitzgerald Email: lindy.fitzgerald@uwa.edu.au Tel: 61 8 6488 2353, Fax: 61 8 6488 7527

Abstract

Following neurotrauma, cells beyond the initial trauma site undergo secondary degeneration, with excess Ca^{2+} a likely trigger for loss of neurons, compact myelin and function. Treatment using inhibitors of specific Ca^{2+} channels has shown promise in preclinical studies, but clinical trials have been disappointing and combinatorial approaches are needed. We assessed efficacy of multiple combinations of three Ca^{2+} channel inhibitors at reducing secondary degeneration following partial optic nerve transection in rat. We used lomerizine to inhibit voltage gated Ca^{2+} channels; oxidised adenosine-triphosphate (oxATP) to inhibit purinergic $P2X_7$ receptors and/or 2-[7-(1H-imidazol-1-yl)-6-nitro-2,3-dioxo-1,2,3,4-tetrahydro quinoxalin-1-yl]acetic acid (INQ) to inhibit Ca^{2+} permeable α-amino-3-hydroxy-5-methyl-4-isoxazolepropionic acid (AMPA) receptors. Only the three Ca^{2+} channel inhibitors delivered in combination significantly preserved visual function, as assessed using the optokinetic nystagmus visual reflex, at 3 months after injury. Preservation of retinal ganglion cells was partial and is unlikely to have accounted for differential effects on function. A range of the Ca^{2+} channel inhibitor combinations prevented swelling of optic nerve vulnerable to secondary degeneration. Each of the treatments involving lomerizine significantly increased the proportion of axons with normal compact myelin. Nevertheless, limiting decompaction of myelin was not sufficient for preservation of function in our model. Multiple combinations of Ca^{2+} channel inhibitors reduced formation of atypical node / paranode complexes; outcomes were not associated with preservation of visual function. However, prevention of lengthening of the paranodal gap that was only achieved by treatment with the three Ca^{2+} channel inhibitors in combination was an important additional effect that likely contributed to the

associated preservation of the optokinetic reflex using this combinatorial treatment strategy.

Keywords: Secondary degeneration; Ca^{2+} channel inhibitors; myelin; myelin compaction; neurotrauma; visual system; node / paranode complex; oxidative stress

Abbreviations: 2-[7-(1H-imidazol-1-yl)-6-nitro-2,3-dioxo-1,2,3,4-tetrahydro quinoxalin-1-yl]acetic acid, INQ; α-amino-3-hydroxy-5-methyl-4-isoxazolepropionic acid, AMPA; adenosine triphosphate, ATP; intraperitoneally, i.p.; lomerizine, Lom; N-methyl-D-aspartic acid, NMDA; optical cutting temperature, OCT; oligodendrocyte precursor cells, OPCs; optic nerve, ON; oxidised adenosine-triphosphate, oxATP; paraformaldehyde, PFA; partial transection, PT; phosphate buffered saline, PBS; retinal ganglion cell, RGC; standard error of the mean, SEM; transmission electron microscopy, TEM; voltage-gated calcium channels, VGCCs.

1. Introduction

Following traumatic injury to the central nervous system (CNS), cells in the lesion site invariably die rapidly, and their function is lost (Norenberg et al., 2004). Nearby and remote neurons and glia initially spared by the lesion are vulnerable to bystander damage, known as secondary degeneration, resulting in further loss of neurons, myelin and function (Crowe et al., 1997; Levkovitch-Verbin et al., 2003; Khodorov, 2004; Farkas and Povlishock, 2007; Lasiene et al., 2008; Arvanian et al., 2009). Secondary degeneration is initiated by a cascade of reactive metabolic events including glutamate-excitotoxicity, Ca^{2+} overload, excess free radical formation, oxidative stress and reduced adenosine triphosphate (ATP) production, which lead to cell death (Camello-Almaraz et al., 2006; Giaume et al., 2007; Fitzgerald et al., 2010; Lau and Tymianski, 2010; Peng and Jou, 2010). Myelinating oligodendrocytes and oligodendrocyte precursor cells (OPCs) are particularly sensitive to excitotoxic insult and oxidative stress, due to their high lipid content and low levels of antioxidants, with sensitivity dependent on maturation status (Back et al., 1998; Juurlink et al., 1998; Micu et al., 2006; Saggu et al., 2010). The compact layers of myelin are vulnerable to reactive oxygen species and lipid peroxidation, which is elevated during secondary degeneration (McTigue and Tripathi, 2008), and associated with myelin decompaction (Payne et al., 2011, 2012). Rescuing intact, but vulnerable, tissue from secondary death is recognised as the only feasible way to minimise adverse sequelae and improve long term functional outcomes after CNS trauma (Crowe et al., 1997; Blair et al., 2005).

Redistribution of Ca^{2+} is thought to be a key trigger of secondary degeneration (Lobsiger and Cleveland, 2007; Knoferle et al., 2010; Wells et al., 2012). Normal

intracellular Ca^{2+} homeostasis is impaired following injury, with increased concentration of cytosolic Ca^{2+} through Ca^{2+} influx from extracellular pools, leading to further elevations *via* release from intracellular stores (Paschen, 2001; Syntichaki and Tavernarakis, 2003; Weber, 2012). Voltage-gated Ca^{2+} channels (VGCCs) are able to facilitate both extracellular Ca^{2+} influx and intracellular release of Ca^{2+} into the cytosol and are considered critical for the initial Ca^{2+} signaling observed after neurotrauma (Imaizumi et al., 1999; Weber, 2012). Purinergic $P2X_7$ receptors may also contribute to excess Ca^{2+} influx as they are upregulated following injury in response to released ATP (Franke et al., 2004; Hamilton et al., 2008). $P2X_7$, AMPA and N-methyl-D-aspartic acid (NMDA) receptor activation in OPCs and oligodendrocytes has been implicated in various forms of white matter injury (Li et al., 2000; Stevens et al., 2002; Karadottir et al., 2005; Salter and Fern, 2005; Matute et al., 2007; Pitt et al., 2010), associated with disruptions to axoglial junction and node and paranode domains, resulting in failure of saltatory conduction (Fu et al., 2009; Rosenbluth, 2009; Buttermore et al., 2011).

The effects of inhibition of Ca^{2+} channels implicated in secondary degeneration have been assessed in preclinical studies. Lomerizine dihydrochloride (lomerizine) is a relatively CNS specific L - and T - type VGCC inhibitor already in use as an anti - migraine agent (Hara et al., 1999; Toriu et al., 2000; Tamaki et al., 2003). Lomerizine protects RGCs in animal models of ischemia, hypoxia and secondary death (Hara et al., 1999; Toriu et al., 2000; Karim et al., 2006), limiting elevations in cytosolic Ca^{2+} concentrations (Yamada et al., 2006). We have previously shown that lomerizine protects retinal ganglion cell (RGC) axons and somata vulnerable to secondary degeneration *in vivo* following partial optic nerve (ON) transection, but has limited

effects on visual function (Fitzgerald et al., 2009a; Selt et al., 2010). Similarly, blockade of ATP - gated $P2X_7$ receptors *via* the irreversible, non - competitive antagonist oxATP limits Ca^{2+} flux in several models of CNS dysfunction and protects against secondary damage following spinal cord injury (Wang et al., 2004; Choi et al., 2007; Kennedy, 2007; Matute et al., 2007). The novel Ca^{2+} - permeable AMPA receptor competitive antagonist INQ has the advantage of high solubility and has shown therapeutic potential in preclinical studies of ischemia (Takahashi et al., 2002). INQ may also prevent activation of the NMDA receptor and VGCCs (Miller, 1991; Wong and Kemp, 1991) and reversal of the Na^+ - Ca^{2+} exchanger (Takahashi et al., 2002).

However, clinical trials with these and other single Ca^{2+} channel inhibitors for treatment of CNS injury have been disappointing (Takahashi et al., 2002; Muir, 2006; Klein and Engelhard, 2010), and while combinatorial treatments are now widely acknowledged as necessary to successfully combat secondary degeneration following neurotrauma (Coleman, 2005; Miller and Mi, 2007), few studies addressing effects of combinations of Ca^{2+} channel inhibitors have been reported. Here we have used the partial ON transection model of secondary degeneration *in vivo* (Levkovitch-Verbin et al., 2003; Fitzgerald et al., 2009a) and assessed the effects of three Ca^{2+} channel inhibitors in combination. We used combinations of lomerizine, oxATP and / or INQ, assessing visual function, neuroprotection, myelin compaction, and structure of node of Ranvier / paranode complexes, at 3 months after injury.

2. Materials and methods

2.1 Animals

Female Piebald Virol Glaxo (PVG) adult rats (160 - 200 g), obtained from the Animal Resource Centre (Murdoch, Western Australia), were housed in groups of three under standard conditions including 12 h light / dark cycles and *ad libitum* access to chow and water. All procedures were approved by The University of Western Australia Animal Ethics Committee and all efforts were made to minimise animal suffering and reduce the number of animals used; alternatives to *in vivo* techniques were not suitable for a study of this nature. Anaesthesia was administered intraperitoneally (i.p.) as a combination of Xylazine (Ilium Xylazil 20, 10 mg / kg) and Ketamine (Ketamil, 50 mg / kg, Troy Laboratories). Partial transection (PT) of ON, in which RGC axons in the dorsal aspect of the ON are lesioned leaving those on the ventral side intact (but susceptible to secondary degeneration), was conducted as described previously (Fitzgerald et al., 2009a). Briefly, approximately 1 mm behind the eye, the dorsal side of the right ON was partially transected to a controlled depth of 200 µm using a diamond radial keratotomy knife (Geuder). Post-operative analgesia was administered (2.8 mg/kg carprofen, Norbrook). Controls were uninjured normal animals as sham injured animals have been shown to be no different to normals in terms of visual function, RGC numbers and other cellular parameters (Fitzgerald et al., 2009a).

2.2 Treatments

Test animals (n = 7 – 10 / group, total study n = 93) were split into groups for testing of combinations of three Ca^{2+} channel inhibitors, lomerizine dihydrochloride (lomerizine or Lom; LKT Labs), oxATP (Sigma) and/ or INQ (synthesised as

described below). Choice of treatment durations and concentrations were based on previously published studies using these agents individually. Lomerizine in butter (30 mg / kg, (Tamaki et al., 2003)) or butter alone was administered orally to all animals, while the animals were gently held. Treatment began on the day of surgery after recovery from anaesthesia and continued twice daily for 3 months (6 days / week). OxATP (1 mM, (Matute et al., 2007)) and / or INQ (240 µM, based on continued delivery of the 1 µg administered as a single bolus by (King and Barr, 2007)) dissolved in phosphate buffered saline (PBS), were delivered for the first 2 weeks after injury at a rate of 0.5 µL / h *via* a subcutaneously implanted, pre-loaded mini-osmotic pump (Model 2002, Alzet) (Beazley et al., 1996; Matute, 1998), attached to a cannula targeting the dorsal aspect of the ON dura mater. Longer duration of treatment with oxATP and / or INQ was not possible due to the 2 week maximum implant time of the mini - osmotic pumps for optimal efficacy. The volumes remaining in the mini - osmotic pumps were assessed after surgical removal and found to correspond with the predicted delivered volume. Rats were housed individually to minimise disturbance by cage-mates, until pumps were surgically removed at 2 weeks after injury. Additional groups of animals were included in the study design to control for isolation, and further controls included injured animals treated with vehicle only (PBS in pumps), injured animals without pumps but treated with butter vehicle only (control for lomerizine vehicle) and completely normal animals (n = 7 - 10 for all groups). Outcomes were assessed at 3 months after injury. A separate cohort of animals, for selected treatments only (n = 4 - 5 / group), were assessed for oxidative stress at 2 days after injury.

INQ was synthesised using a previously reported procedure with slight modifications to steps 2 and 3 (Shishikura et al., Yamanouchi Pharmaceuticals Co., Ltd., (2000) *1,2,3,4-Tetrahydroquinoxalinedione Derivative,* U.S. Pat. 6,096,743). The structure and purity of the final compound was confirmed by nuclear magnetic resonance (^{1}H NMR) analysis in deuterated DMSO: δ_H (500 MHz, DMSO-d6) 4.89 (s, 2H), 7.88 (s, 1H), 8.01 (s, 1H), 8.08 (s, 1H), 8.28 (s, 1H), 9.43 (s, 1H), 12.89 (s, 1H), 13.1-14.2 (bs, 1H). Modifications to Step 2 (reduction of N-(2-nitro-5-fluorophenyl)glycine ethyl ester to N-(2-amino-5-fluorophenyl)glycine ethyl ester) were tetrahydrofuran was distilled prior to use; methanol was dried over magnesium sulphate and stored over molecular sieves prior to use. The hydrogenation reaction was stirred at room temperature for 1.5 h and monitored by thin layer chromatography (diethylether: methanol 10:1). The reaction mixture was then filtered through celite and concentrated under reduced pressure. The resulting crude product was purified by loading onto a short plug of silica, the silica plug was initially washed with ethyl acetate to remove impurities and then with methanol to collect the product, N-(2-amino-5-fluorophenyl)glycine ethyl ester, in 20 % yield. Modifications to step 3 (acylation of N-(2-amino-5-fluorophenyl)glycine ethyl ester to ethyl 2-(7-fluoro-2,3-dioxo-1,2,3,4-tetrahydroquinoxalin-1-yl)acetate), were chloroform was dried as for methanol above and the crude product purified as for step 2, to collect the product, ethyl 2-(7-fluoro-2,3-dioxo-1,2,3,4-tetrahydroquinoxalin-1-yl)acetate, in quantitative yield.

2.3 Optokinetic nystagmus

Three months post-surgery, all rats were anaesthetised as above and their uninjured left eye lids sutured shut (6-0 silk) to ensure that behavioural responses observed were

due to the visual ability of the injured ON. Following complete recovery from anaesthesia (next day), behavioural testing was conducted using the optokinetic nystagmus test as described previously, including use of similar numbers of animals / treatment group (Abdeljalil et al., 2005; Fitzgerald et al., 2009a). Briefly, after acclimatisation, responses of rats to rotation of black and white stripes in the anti - clockwise direction were recorded. Analysis of recorded footage was performed by three independent observers who counted the number of smooth pursuits and fast resets within the period each rat was engaged in the task; data were averaged for the three observers.

There was no significant difference in optokinetic nystagmus responses between PT injured animals implanted with a mini - osmotic pump delivering PBS and those without the implant (assessed by direct statistical comparison of these two groups using Student's t-test, $p > 0.05$), allowing pooling of groups referred to as 'vehicle' (i.e. PBS and / or butter vehicle) for this outcome measure. Similarly, responses from animals of treatment groups without a pump implanted and housed in groups of 3, were not different from those given the same treatment but kept in isolation for the first 2 weeks, allowing pooling of data from these groups for the behavioural analyses ($p > 0.05$, data not shown). PT injured animals implanted with a mini - osmotic pump delivering PBS and treated with butter vehicle orally were used as the vehicle control for all other outcome measures.

2.4 Tissue preparation

Rats were euthanized with Euthal (Pentobarbitone sodium 850 mg/ kg and Phenytoin sodium 125 mg/ kg; Delvet, i.p.) and transcardially perfused with 0.9% NaCl

followed by 4% paraformaldehyde (Sigma) in 0.1 M phosphate buffer, pH 7.2 (PFA). For each animal, right retinae and ONs were removed and post-fixed overnight in 4% PFA before cryoprotection in 15% sucrose in PBS. For immunohistochemical studies (n = 3 -6 / group), tissue was frozen in optical cutting temperature (OCT) compound and a cryostat (CM1900, Leica) used to cut longitudinal ON sections (14 µm) or sagittal retinal sections (20 µm) which were collected onto Superfrost Plus microscope slides (Menzel-Gläser) and stored at -80°C until use.

A subset of ONs (n = 3 - 4/ group) from selected treatment groups were processed for transmission electron microscopy (TEM) studies as described previously (Payne et al., 2011, 2012). An n = 3 - 4 / group is standard for ultrastructural studies of this nature (Phokeo et al., 2002). Briefly, following perfusion, tissue was processed and sectioned transversely using an LKB Bromma, NOVA Ultrotome®. Sections at the injury site were identified with reference to adjacent semi-thin sections stained with toluidine blue in 1% borax (Scott Scientific), also allowing confirmation of the transverse nature of the sections. Low-power (20X magnification) light microscope images of the toluidine blue stained sections were taken to identify the injury site and vulnerable ventral ON for TEM analysis, and for quantification of ON ventral cross-sectional area. Ultrathin sections (100 nm) of the injury site were mounted on 3.05 mm copper support grids, and post-stained with uranyl acetate and lead citrate for TEM.

2.5 ON morphology quantification

ON diameter was drawn mediolaterally across the nerve, at a location where the arc of the ON was at its widest, when the dorsal lesion was uppermost in the image. The ventral cross-sectional area was measured across the mediolateral diameter and the

remaining ON in an arc like fashion (n = 3 - 4/ group). The neural sheath was excluded from all measurements and analyses were quantified using Fiji analysis software (NIH).

2.6 Immunohistochemistry

Sections were air - dried, washed in PBS, and then PBS + 0.2 % Triton-X 100 for 10 min and incubated at 4°C overnight with primary antibodies (diluted in PBS + 0.2% Triton X100 (PBST) containing 5% normal horse serum) detecting: neurons (anti - β - III tubulin; 1:500, Covance or Abcam); oligodendrocytes (anti - olig1; 1:500, Abcam); Caspr (anti - Caspr; 1:750, Abcam); or carboxy - methyl lysine (CML, anti - CML; 1:500, CosmoBio). Antibody binding was visualised following 2 h incubation at room temperature with appropriate secondary antibodies (Alexa Fluor 488, 555 or 647 all at 1:400 in PBST, Molecular Probes) and Hoechst nuclear stain (1 μg / mL, Invitrogen). Slides were coverslipped using Fluoromount-G (Southern Biotechnology) and viewed using fluorescence microscopy. All sections for each antibody were immunostained at the same time to ensure uniformity of the immunohistochemical procedures, and the images were captured at constant exposure times. Control sections stained only with secondary antibodies were included in all experiments and showed no or only minimal fluorescence (data not shown).

2.7 Immunohistochemistry image analysis and quantification

For analyses of RGCs in retinal sections, retinae were processed and sectioned as described in section 2.4 above. Three representative fields of view in ventral retina (each 100 μm x 100 μm), in 3 retinal sections / animal, were counted by a single, blinded experimenter. As such, 9 fields of view were counted from each animal; n = 6

animals/ control or treatment group. The mean numbers of β - III tubulin+ cells in retinal sections were expressed / mm^2, based on the average width of the ganglion cell layer; statistical analyses for this and all analyses in the current study were conducted using the means from each animal i.e. 'n'. Measures of length of retinal sections taken from the middle of the retina showed no difference between normal (control), PT injured animals or PT injured animals treated with the combination of all three inhibitors (normal = 10.4 ± 0.3 mm, PT injured = 10.4 ± 0.4 mm, PT injured treated = 10.3 ± 0.2 mm; F = 0.07 (DF 2) p = 0.93), indicating that changes in retinal area are unlikely to have impacted on density measures. Further, fields of view were assessed in ventral retina and we find no evidence in the literature of retinal swelling or shrinkage in this region following ON injury.

For quantification of immunointensity in ON sections, the ventral area directly below the primary injury site in a single section/ animal (n = 3 - 6 animals / group) was visualised and photographed using a Nikon Eclipse Ti inverted microscope (Nikon Corporation) with a 20X/1.3 N.A. oil immersion objective. A series of optical images at 0.5 µm increments along the z-axis were acquired from the middle 6 µm of each 14 µm thick section, sampling a field of view of 217.5 x 162.5 µm of the ventral area vulnerable to secondary degeneration. All images were collected using Nikon Elements AT software and deconvoluted using autoquant blind deconvolution. For analyses where colocalisation of 2 markers was assessed, a single image in the z plane with the strongest staining at all wavelengths was used to ensure optimal visualisation and true colocalisation. Mean intensities in defined areas were analysed using ImageJ software (NIH). Representative images of CML and olig1 immunohistochemistry are presented as single images in the z plane.

For assessments of node / paranode complexes, sections were imaged as above and each image stack was opened in ImageJ software (NIH) using the ImageJ ND2 reader plugin, and collapsed into a single image for further analysis as a TIFF file. Typical node / paranode complexes were characterised by a β-III tubulin+ area, also shown to colocalise with $Na_v1.6$ in ON vulnerable to secondary degeneration (unpublished observation), flanked by two Caspr+ clusters (paranodes). For each animal, 30 typical node / paranode complexes were assessed; the length of the paranodal gap, defined as the distance between two Caspr+ paranodes and assumed to reflect the length of the node of Ranvier (Howell et al., 2006), and the average lengths of the flanking paranodes were quantified using ImageJ software.

The numbers of typical and atypical node / paranode complexes in the central 125 x 125 µm area of the fields of view were also quantified. Atypical node / paranode complexes were classified as either hemi - nodes or single paranodes. Hemi - nodes were characterised by a β-III tubulin+ area flanked by only one paranode. Single paranodes were characterised by a Caspr stained cluster not associated with β-III tubulin immunostaining. The presence of single paranodes and hemi-nodes likely reflects disruption to the node / paranode structure such that immunoreactivity is lost. Orthogonal z - projections were used to determine that the depth of typical node / paranode complexes never exceeded more than 3 individual optical images in the z plane. As such, the majority of atypical complexes were present well within the z stacks and the probability that parts of complexes were missing adjacent to the edge of z-stacks was constant across each of the sections assessed.

2.8 TEM image analysis and quantification

For TEM, ultrathin sections were viewed under a Philips CM10 model TEM at 80 kV, 25,000X magnification, and digitally imaged via the Olympus Megaview III digital camera attached to the 35 mm camera port above the TEM viewing screen *via* Olympus iTEM Soft Imaging Solution software. Approximately 0.15 - 0.2% of the total axon population (~150 - 200 axons / animal) were analysed; sampling was in ventral ON and similar to that described in Payne et al (2011), based on a field of view of 440 μm^2.

Axons were classified as having completely normal myelin, marginally-decompacted myelin, abnormal myelin, or as unmyelinated. Normal myelin was thick, of high - electron density, with no signs of decompaction. Axons with marginally decompacted myelin presented small signs of decompaction in $\leq$ 20% of the circumference of the myelin sheath. Axons with abnormal myelin were categorised into two subpopulations: axons with partially-decompacted myelin, characterised by $\geq$ 20% of the myelin sheath showing signs of decompaction; or axons with fully-decompacted myelin, characterised by the entire axon being ensheathed with multiple layers of thin, moderate-electron dense myelin. The densities of axons (relative to their axon type) were expressed as a proportion of the total number of axons counted in ventral ON (mean ± SEM axons).

2.9 Statistical analyses

Results were analysed using the statistical package StatView for Windows (SAS Institute Inc.) or IBM SPSS Statistics. Kolmogorov - Smirnov tests were used to confirm that results were consistent with a normal distribution and equality of

variance F - tests to test for homogeneity of variances in groups within experiments. All data are expressed as means of each treatment group ± SEM. ANOVAs followed by Dunnett's or Games-Howell *post hoc* tests as appropriate were used to statistically compare quantitative measures of each treatment group to the injured vehicle control (animals with PBS delivery of vehicle *via* osmotic mini-pump and butter vehicle orally) or to the group of uninjured, normal animals (ANOVA F test and degrees of freedom (DF), as well as p value from *post hoc* tests are given). Statistical comparisons between individual treatment combinations were not conducted, due to the large number of groups and low n's for some outcome measures precluding attainment of statistical significance using Bonferroni Dunn *post hoc* tests. Student's t - test was used to compare data relating to multiple control groups to facilitate pooling. All statistical tests required $p \leq 0.05$ for significance.

3. Results and Discussion

3.1 Three Ca^{2+} channel inhibitors in combination preserved visual function

As previously reported (Selt et al., 2010; Payne et al., 2012), partial ON transection resulted in a significant reduction in the number of optokinetic nystagmus responses at 3 months after injury (Fig.1: smooth pursuits $F = 3.26$ (DF 8) $p \leq 0.05$; fast resets $F = 2.43$ (DF 8) $p \leq 0.05$). However, treatment of injured rats with the combination of all three selected Ca^{2+} channel inhibitors together (Lom / oxATP / INQ) resulted in complete preservation of both the number of smooth pursuits and fast resets, to levels significantly higher than rats receiving the vehicle alone (Fig.1: smooth pursuits $F = 3.26$ (DF 8) $p \leq 0.05$; fast resets $F = 2.43$ (DF 8) $p \leq 0.05$), and not different from normal uninjured animals ($p > 0.05$). These results demonstrate that the loss of function, due to both the axotomy itself and the consequent loss of glia at the primary injury, can be overcome by sustained inhibition of Ca^{2+} flux through VGCCs together with early inhibition *via* $P2X_7$ and AMPA receptors. This is presumably due to limiting of secondary degeneration, as explored further below. Animals treated with all other combinations of Ca^{2+} channel inhibitors made intermediate numbers of responses, neither significantly improved above the vehicle control nor different from normal animals ($p > 0.05$), except for smooth pursuits by rats treated with oxATP alone ($p \leq 0.05$). Note that throughout the current study we do not directly compare the different treatment combinations to each other, merely each treatment combination to vehicle treated or normal controls. As such, the effectiveness of the triple Ca^{2+} channel inhibitor combination in comparison to the other combinations cannot be commented on, except that it is the only treatment to result in statistically significant improvements in visual function from vehicle treated controls. We did not include control groups to assess the effects of the treatment combinations on normal uninjured

animals due to the large number of additional groups that would be required; we are not aware of any evidence to indicate that the presence of the various drug combinations alters parameters in rats that received no injury.

3.2 Retinal ganglion cells were not fully protected

As previously reported (Selt et al., 2010), partial ON transection resulted in significant loss of RGCs in ventral retina (Fig. 2A: $F = 1.96$ (DF 8) $p \leq 0.05$), demonstrated to be as a direct consequence of secondary degeneration (Fitzgerald et al., 2009b). While no combination of Ca^{2+} channel inhibitors significantly increased RGC density in ventral retina compared to vehicle treated animals, all inhibitor combinations were also not significantly different to normal, indicating an intermediate RGC density as a result of each of the tested treatment combinations (Fig. 2A, $F = 1.96$ (DF 8) $p > 0.05$). We have previously reported that 1 month of lomerizine treatment protected RGCs when assessed at the conclusion of treatment, but that protection was not sustained when assessed at 3 months (Selt et al., 2010). The present findings add to these and indicate that sustained administration of lomerizine is still insufficient to completely protect RGCs at 3 months after injury.

Similarly, axon density, as measured by β - III tubulin immunointensity in ventral ON in the section at the injury site, was significantly reduced following partial transection (Fig. 2B, $F = 2.91$ (DF 5) $p \leq 0.05$). Ventral ON axons escape the primary injury (dorsal) but are vulnerable to secondary degeneration (Fitzgerald et al., 2009a). We assessed the effects of a subset of the treatments on β - III tubulin immunointensity, as a measure of axonal protection. Treatment of injured rats with the combination of all three Ca^{2+} channel inhibitors together (Lom / oxATP / INQ) resulted in complete

preservation of β - III tubulin+ axonal profiles, to levels significantly higher than rats receiving the vehicle alone (Fig.2B, $F = 2.91$ (DF 5) $p \leq 0.05$), and not different from normal uninjured animals ($p > 0.05$). No other tested combination of Ca^{2+} channel inhibitors resulted in significant preservation of β - III tubulin+ axonal profiles compared to vehicle treated animals; however treatments were also not different to normal ON, again indicating intermediate effects. As such, while optokinetic nystagmus responses and axonal density were completely preserved by treatment with the three Ca^{2+} channel inhibitors in combination, RGC somata were not. RGC axons and somata may have differing responses to combinations of Ca^{2+} channel inhibitors, although differences in the sensitivity of detection of improvements may be a contributing factor. Taken together, our results imply that preservation of RGCs is unlikely to have accounted for the differential effects of the various combinations of Ca^{2+} channel inhibitors on function.

3.3 Optic nerve swelling prevented by combinations of Ca^{2+} channel inhibitors

The ventral half of the ON swelled significantly as a consequence of secondary degeneration (Fig. 3A, B, D; $F = 3.30$ (DF 5) $p \leq 0.05$), as previously reported (Selt et al., 2010; Payne et al., 2011). We assessed ventral ON area following treatment with selected combinations of Ca^{2+} channel inhibitors, as a prequel to TEM analyses, and demonstrated that ventral ON area was significantly reduced compared to injured, vehicle treated animals following treatment with the Lom, Lom / INQ, or oxATP / INQ combinations ($p \leq 0.05$), with treatment with Lom / oxATP / INQ approaching a statistically significant reduction ($p=0.07$). Furthermore, this reduction in swelling was such that ventral ON area was not significantly different from normal (Fig. 3D, $p > 0.05$). Our data indicate that it is the control of excess intracellular Ca^{2+}

concentrations that is important for prevention of swelling of ON vulnerable to secondary degeneration, rather than downstream signalling pathways of specific Ca^{2+} channels or receptors, as lomerizine alone was equally as effective as the oxATP / INQ combination. Furthermore, as the oxATP / INQ treatment combination was only delivered for the first 2 weeks after injury, it is likely that early rather than chronic inhibition of excess Ca^{2+} flux is important for control of swelling of nerve vulnerable to secondary degeneration. Swelling of CNS tissue after injury is associated with astrocyte hypertrophy, inflammatory cell infiltration and extracellular matrix remodelling (Sykova and Vargova, 2008; Saadoun and Papadopoulos, 2010), and we have demonstrated astrocyte hypertrophy associated with oxidative stress as early as 5 minutes after injury in ON vulnerable to secondary degeneration (Fitzgerald et al., 2010). Nevertheless, Ca^{2+} channel inhibition initiated some hours after injury (e.g. lomerizine alone), was effective at limiting chronic ON swelling, indicating that a therapeutic window exists for Ca^{2+} channel inhibitors as a strategy to prevent swelling of a white matter tract.

3.4 Myelin decompaction reduced by combinations of Ca^{2+} channel inhibitors

Similar to previous reports (Payne et al., 2011, 2012), at 3 months following partial ON transection, the density of axons ensheathed in normal compact myelin, expressed as a proportion of the total number of axons assessed in ventral ON, was significantly reduced (Fig. 4A – C, $F = 10.08$ (DF 5) $p \leq 0.01$). The proportion of axons with myelin that was marginally or fully decompacted did not significantly change with injury, and nor did the proportion of unmyelinated axons (Fig. 4A, B, $F = 2.71$ (DF 5) and $F = 1.57$ (DF 5) respectively, $p > 0.05$). However, as expected, there was a significant increase in the proportion of axons with partially decompacted myelin

vulnerable to secondary degeneration, at 3 months after injury (Fig. 4A, B, D, $F = 9.95$ (DF 5) $p \leq 0.01$). The proportion of axons with partially decompacted myelin was slightly higher here than in our previous studies (Payne et al., 2011, 2012), due to the increased magnification of the current TEM images allowing better detection of separated myelin lamellae and decompaction.

Selected combinations of Ca^{2+} channel inhibitors were used to treat animals following partial ON transection for ultrastructural assessments of myelin. Electron microscopy analyses of myelin compaction are laborious and we therefore limited our analyses to selected combinations encompassing a range of treatments likely to be of interest based on functional outcomes. It was shown that treatments involving lomerizine significantly increased the proportion of axons with normal compact myelin compared to injured, vehicle treated animals (Fig. 4B, C, $F = 10.08$ (DF 5) $p \leq 0.01$), to levels not different from normal ($p > 0.05$) at 3 months after injury. Correspondingly, treatments involving lomerizine decreased the proportion of axons with partially decompacted myelin compared to injured, vehicle treated animals (Fig. 4B, D, $F = 9.95$ (DF 5) $p \leq 0.01$), to levels not different from normal ($p > 0.05$). None of the tested treatment combinations affected the proportions of axons with marginally decompacted or fully decompacted myelin, or of unmyelinated axons, when compared to ON from vehicle treated animals or normal ON ($p > 0.05$, data not shown).

While treatment with the oxATP / INQ combination did not significantly increase the proportion of axons with normal compact myelin ($p > 0.05$), it did decrease the proportion of axons with partially decompacted myelin (Fig. 4C, D, $p \leq 0.01$) compared to injured, vehicle treated axons. However, the proportions of axons with

partially decompacted myelin also remained significantly different from normal (Fig. 4D, $p \leq 0.03$), indicating an intermediate effect. This may have been due to the shorter treatment duration with these agents (2 weeks), rather than an indication of the importance of inhibiting VGCCs over $P2X_7$ or AMPA receptors. As such, it is possible that sustained treatment with oxATP / INQ may have resulted in more pronounced reductions in myelin decompaction. Nevertheless, sustained inhibition of VGCCs effectively reduced myelin decompaction, implying that the control of intracellular Ca^{2+} concentration, either directly entering cells through VGCCs or downstream *via* VGCC depolarisation-dependent ryanodine receptor mediated release from the endoplasmic reticulum (Calin-Jageman and Lee, 2008), is important in preserving myelin integrity. Limiting excess cytosolic Ca^{2+} is likely to reduce free radical species, resultant oxidative stress and lipid peroxidation in oligodendrocytes (Kaptanoglu et al., 2004), leading to reduced myelin abnormalities such as decompaction in ON vulnerable to secondary degeneration (Bizzozero et al., 2004).

The preservation of compact myelin and the reductions in the proportions of axons with partially decompacted myelin following treatment with the triple combination of Ca^{2+} channel inhibitors was associated with preservation of visual function. However, while treatment with Lom or Lom / INQ was essentially equally as effective at reducing myelin decompaction as the 3 agents in combination, they did not fully preserve vision, as assessed by optokinetic nystagmus, at 3 months. Therefore, limiting the decompaction of myelin was not sufficient to maintain function, in our model.

3.5 Length of paranodal gap preserved by three Ca^{2+} channel inhibitors in combination

Myelin decompaction is likely to be associated with alterations in the structure of axoglial junctions and the node / paranode complex (Dupree et al., 1998; Nave, 2010). As such, we quantified structural parameters of the nodes and paranodes in ventral ON vulnerable to secondary degeneration, following partial ON transection and treatment with the same selected combinations of Ca^{2+} channel inhibitors as those used for the TEM assessments of myelin compaction. We assessed lengths of nodes of Ranvier indirectly, as the distance between Caspr+ paranodes (Einheber et al., 1997) in typical node / paranode complexes, which in our hands corresponds to the length of $Na_v1.6$+ regions in normal ON (not shown); an approach that has been used with other paranodal markers (Howell et al., 2006). In ventral ON vulnerable to secondary degeneration, the paranodal gap, referred to hereafter as the node length, was significantly increased compared to normal ON, at 3 months after injury (Fig. 5A, $F = 7.36$ (DF 5) $p \leq 0.05$). Of the assessed treatments, only the Lom / oxATP / INQ triple Ca^{2+} channel inhibitor combination resulted in significantly decreased node length in ventral ON compared to injured, vehicle treated animals ($p \leq 0.01$), to levels not significantly different from normal (Fig. 5A, $p > 0.05$). Node lengths in animals treated with Lom / INQ following injury were not significantly different to either node lengths in ventral ON from vehicle treated animals or from normal animals (Fig. 5A, $p > 0.05$), indicating an intermediate effect and implying the additional requirement of oxATP for complete prevention of node lengthening. The remaining tested combinations of Ca^{2+} channel inhibitors (Lom, oxATP / INQ) did not preserve normal node length in injured animals, as node lengths were not significantly different to

levels in injured, vehicle treated animals ($p > 0.05$), and were significantly increased compared to nodes in normal ON (Fig. 5A, $p \leq 0.05$).

Taken together, our results indicate that prevention of myelin decompaction by Ca^{2+} channel inhibitor treatment combinations including lomerizine did not necessarily result in prevention of node lengthening. However, there was an association between preservation of node length and axonal density, indicating the importance of preservation of the clustering of ion channels at the node of Ranvier for maintenance of axons, or *vice versa*. The average length and width of paranodes did not change as a result of injury in ventral ON at 3 months, nor was there an effect of any of the tested treatment combinations (data not shown, $F = 3.07$ (DF 5) and $F = 1.52$ (DF 5) respectively, $p > 0.05$).

Maintenance of normal node length in ON vulnerable to secondary degeneration is likely to result in improved saltatory conduction and preservation of function (Rosenbluth, 2009; Buttermore et al., 2011). Indeed, the only tested combination of Ca^{2+} channel inhibitors to effectively limit changes in the length of the node of Ranvier (Lom / oxATP / INQ) was also the only treatment combination to fully preserve visual function. Neither sustained inhibition of VGCCs with lomerizine treatment alone nor sustained inhibition of VGCCs accompanied by early inhibition of AMPA receptors with INQ, were fully effective at preserving node length. Additional early inhibition of excess Ca^{2+} flux through both $P2X_7$ and AMPA receptors is likely to be required, although our study design limits interpretation such that we cannot discount the possibility that lomerizine in combination with early oxATP treatment may also significantly reduce node length. Over - activation of AMPA receptors can

lead to reversal of the Na^+ - Ca^{2+} exchanger and subsequent activation of calpains, which are proteases that have been linked to myelin degradation (Yanagisawa et al., 1988; Araujo et al., 2007). Taken together our results indicate that control of excess Ca^{2+} flux *via* VGCCs and $P2X_7$ receptors, (Miller, 1991), and likely also *via* inhibition of AMPA receptor - dependent processes, appears to be necessary for control of node structure and associated preservation of visual function.

3.6 Atypical node / paranode complexes and oxidative stress reduced by combinations of Ca^{2+} channel inhibitors

The presence of atypical node / paranode complexes in ON vulnerable to secondary degeneration was confirmed using orthogonal projections to confirm that missing Caspr+ paranodes were not merely due to node / paranode complexes projecting out of the z stack of collected images (Figure 5B, example single paranode in centre of z stack, boxed). The number of node / paranode complexes that were of atypical morphology (both hemi - nodes and single paranodes), expressed as a percentage of the total number of node / paranode complexes, in ventral ON at 3 months following injury, was significantly increased compared to normal ON (Fig. 5C, $F = 12.07$ (DF 5) $p \leq 0.01$). Interestingly, all of the tested Ca^{2+} channel inhibitor combinations (Lom, Lom / INQ, oxATP / INQ, and Lom / oxATP / INQ) significantly decreased the percentage of atypical node / paranode complexes in ventral ON compared to injured, vehicle treated animals (Fig. 5C, $p \leq 0.01$), and the percentages following treatment with all but Lom / INQ were not significantly different from normal ($p > 0.05$). Increases in atypical node / paranode complexes may be a result of temporary aberrant oligodendrocyte contacts during internodal remodelling and attempted myelin repair following injury (Bhat et al., 2001; Howell et al., 2006). Our results indicate that

control of intracellular Ca^{2+} concentration, regardless of downstream signalling events, is sufficient to prevent formation of these atypical node / paranode structures.

A separate cohort of animals was used to assess CML immunoreactivity, an advanced glycation end-product indicative of oxidative stress (Fu et al., 1996), in controls and following selected treatments of ON vulnerable to secondary degeneration, 2 days after partial ON transection. The increase in CML immunoreactivity in vehicle treated ventral ON vulnerable to secondary degeneration was significantly reduced following treatment with both tested treatments (Lom / INQ and Lom / oxATP / INQ) (Fig. 6A, B, $F = 5.91$ (DF 3) $p \leq 0.05$), and was not different to normal ON ($p > 0.05$). CML immunoreactivity appeared to colocalise with olig1+ oligodendrocyte lineage cells (Fig. 6B). The inhibition of early oxidative stress by both tested Ca^{2+} channel inhibitor combinations indicates that it was not selective inhibition of early production of advanced glycation end-products by only the Lom / oxATP / INQ combination, that resulted in prevention of node lengthening by the triple combination, in ON vulnerable to secondary degeneration (Fig. 5A).

4. Conclusions

We used a combinatorial treatment strategy utilising three Ca^{2+} channel inhibitors in combination to inhibit VGCCs, $P2X_7$ and Ca^{2+} permeable AMPA receptors, in ON vulnerable to secondary degeneration. The combination of the three Ca^{2+} channel inhibitors effectively preserved axonal density and reduced: ON swelling; the proportion of axons with decompacted myelin; the length of the paranodal gap; the percentage of atypical node / paranode structures and an indicator of oxidative stress, all associated with full preservation of visual function, as assessed by optokinetic

nystagmus. No other tested combination of these three inhibitors was able to achieve all of these outcomes and fully protect function (summarised in Table 1). No indications of toxicity were observed in any of the treated animals. Our findings may be applicable to injury to white matter tracts of the central nervous system in general and future studies to assess effects of treatment combinations on functional and cellular responses specific to other clinically relevant models of injury are warranted. A limitation of the current study was the relatively short duration of delivery of the oxATP and INQ treatments (2 weeks), compared to longer term orally administered lomerizine. Intrathecal delivery is required for therapeutics that do not cross the blood brain barrier, and this delivery mode is limited by practical and surgical considerations. As such, strategies to allow sustained delivery of therapeutics *via* nanotechnologies or matrices at the site of injury may be of value in allowing longer term administration of oxATP and / or INQ.

Acknowledgments

This work was supported by the Neurotrauma Research Program (Western Australia) and the National Health and Medical Research Council (NH&MRC, Grant ID: 572550). Our funding sources played no role in the conduct of the research or preparation of this article. We thank Mr. Michael Archer for technical assistance with electron microscopy, Dr K. Swaminathan Iyer for advice regarding synthesis of INQ and Ms Sophie C. Payne for helpful discussions and critical review of the manuscript.

References

Abdeljalil, J., Hamid, M., Abdel-Mouttalib, O., Stephane, R., Raymond, R., Johan, A., Jose, S., Pierre, C., Serge, P. 2005. The optomotor response: a robust first-line visual screening method for mice. Vision Res. 45, 1439-1446.

Araujo, I.M., Carreira, B.P., Pereira, T., Santos, P.F., Soulet, D., Inacio, A., Bahr, B.A., Carvalho, A.P., Ambrosio, A.F., Carvalho, C.M. 2007. Changes in calcium dynamics following the reversal of the sodium-calcium exchanger have a key role in AMPA receptor-mediated neurodegeneration via calpain activation in hippocampal neurons. Cell Death Differ. 14, 1635-1646.

Arvanian, V.L., Schnell, L., Lou, L., Golshani, R., Hunanyan, A., Ghosh, A., Pearse, D.D., Robinson, J.K., Schwab, M.E., Fawcett, J.W., Mendell, L.M. 2009. Chronic spinal hemisection in rats induces a progressive decline in transmission in uninjured fibers to motoneurons. Exp Neurol. 216, 471-480.

Back, S.A., Gan, X., Li, Y., Rosenberg, P.A., Volpe, J.J. 1998. Maturation-dependent vulnerability of oligodendrocytes to oxidative stress-induced death caused by glutathione depletion. J Neurosci. 18, 6241-6253.

Beazley, L.D., Tennant, M., Dunlop, S.A. 1996. The effect of a chronic breakdown of the blood-optic nerve barrier on the severed optic nerve in adult rat. Restor Neurol Neurosci. 10, 95-101.

Bhat, M.A., Rios, J.C., Lu, Y., Garcia-Fresco, G.P., Ching, W., St Martin, M., Li, J., Einheber, S., Chesler, M., Rosenbluth, J., Salzer, J.L., Bellen, H.J. 2001. Axon-glia interactions and the domain organization of myelinated axons requires neurexin IV/Caspr/Paranodin. Neuron. 30, 369-383.

Bizzozero, O.A., DeJesus, G., Howard, T.A. 2004. Exposure of rat optic nerves to nitric oxide causes protein S-nitrosation and myelin decompaction. Neurochem Res. 29, 1675-1685.

Blair, M., Pease, M.E., Hammond, J., Valenta, D., Kielczewski, J., Levkovitch-Verbin, H., Quigley, H. 2005. Effect of glatiramer acetate on primary and secondary degeneration of retinal ganglion cells in the rat. Invest Ophthalmol Vis Sci. 46, 884-890.

Buttermore, E.D., Dupree, J.L., Cheng, J., An, X., Tessarollo, L., Bhat, M.A. 2011. The cytoskeletal adaptor protein band 4.1B is required for the maintenance of paranodal axoglial septate junctions in myelinated axons. J Neurosci. 31, 8013-8024.

Calin-Jageman, I., Lee, A. 2008. Ca(v)1 L-type Ca2+ channel signaling complexes in neurons. J Neurochem. 105, 573-583.

Camello-Almaraz, M.C., Pozo, M.J., Murphy, M.P., Camello, P.J. 2006. Mitochondrial production of oxidants is necessary for physiological calcium oscillations. J Cell Physiol. 206, 487-494.

Choi, H.B., Ryu, J.K., Kim, S.U., McLarnon, J.G. 2007. Modulation of the purinergic P2X7 receptor attenuates lipopolysaccharide-mediated microglial activation and neuronal damage in inflamed brain. J Neurosci. 27, 4957-4968.

Coleman, M. 2005. Axon degeneration mechanisms: commonality amid diversity. Nat Rev Neurosci. 6, 889-898.

Crowe, M.J., Bresnahan, J.C., Shuman, S.L., Masters, J.N., Beattie, M.S. 1997. Apoptosis and delayed degeneration after spinal cord injury in rats and monkeys. Nat Med. 3, 73-76.

Dupree, J.L., Coetzee, T., Blight, A., Suzuki, K., Popko, B. 1998. Myelin galactolipids are essential for proper node of Ranvier formation in the CNS. J Neurosci. 18, 1642-1649.

Einheber, S., Zanazzi, G., Ching, W., Scherer, S., Milner, T.A., Peles, E., Salzer, J.L. 1997. The axonal membrane protein Caspr, a homologue of neurexin IV, is a component of the septate-like paranodal junctions that assemble during myelination. J Cell Biol. 139, 1495-1506.

Farkas, O., Povlishock, J.T. 2007. Cellular and subcellular change evoked by diffuse traumatic brain injury: a complex web of change extending far beyond focal damage. Prog Brain Res. 161, 43-59.

Fitzgerald, M., Bartlett, C.A., Evill, L., Rodger, J., Harvey, A.R., Dunlop, S.A. 2009a. Secondary degeneration of the optic nerve following partial transection: the benefits of lomerizine. Exp Neurol. 216, 219-230.

Fitzgerald, M., Bartlett, C.A., Harvey, A.R., Dunlop, S.A. 2010. Early events of secondary degeneration after partial optic nerve transection: an immunohistochemical study. J Neurotrauma. 27, 439-452.

Fitzgerald, M., Payne, S.C., Bartlett, C.A., Evill, L., Harvey, A.R., Dunlop, S.A. 2009b. Secondary retinal ganglion cell death and the neuroprotective effects of the calcium channel blocker lomerizine. Invest Ophthalmol Vis Sci. 50, 5456-5462.

Franke, H., Gunther, A., Grosche, J., Schmidt, R., Rossner, S., Reinhardt, R., Faber-Zuschratter, H., Schneider, D., Illes, P. 2004. P2X7 receptor expression after ischemia in the cerebral cortex of rats. J Neuropathol Exp Neurol. 63, 686-699.

Fu, M.X., Requena, J.R., Jenkins, A.J., Lyons, T.J., Baynes, J.W., Thorpe, S.R. 1996. The advanced glycation end product, Nepsilon-(carboxymethyl)lysine, is a product of both lipid peroxidation and glycoxidation reactions. J Biol Chem. 271, 9982-9986.

Fu, Y., Sun, W., Shi, Y., Shi, R., Cheng, J.X. 2009. Glutamate excitotoxicity inflicts paranodal myelin splitting and retraction. PLoS One. 4, e6705.

Giaume, C., Kirchhoff, F., Matute, C., Reichenbach, A., Verkhratsky, A. 2007. Glia: the fulcrum of brain diseases. Cell Death Differ. 14, 1324-1335.

Hamilton, N., Vayro, S., Kirchhoff, F., Verkhratsky, A., Robbins, J., Gorecki, D.C., Butt, A.M. 2008. Mechanisms of ATP- and glutamate-mediated calcium signaling in white matter astrocytes. Glia. 56, 734-749.

Hara, H., Shimazawa, M., Sasaoka, M., Yamada, C., Iwakura, Y., Sakai, T., Maeda, Y., Yamaguchi, T., Sukamoto, T., Hashimoto, M. 1999. Selective effects of lomerizine, a novel diphenylmethylpiperazine Ca2+ channel blocker, on cerebral blood flow in rats and dogs. Clinical and experimental pharmacology & physiology. 26, 870-876.

Howell, O.W., Palser, A., Polito, A., Melrose, S., Zonta, B., Scheiermann, C., Vora, A.J., Brophy, P.J., Reynolds, R. 2006. Disruption of neurofascin localization reveals early changes preceding demyelination and remyelination in multiple sclerosis. Brain. 129, 3173-3185.

Imaizumi, T., Kocsis, J.D., Waxman, S.G. 1999. The role of voltage-gated Ca2+ channels in anoxic injury of spinal cord white matter. Brain Research. 817, 84-92.

Juurlink, B.H., Thorburne, S.K., Hertz, L. 1998. Peroxide-scavenging deficit underlies oligodendrocyte susceptibility to oxidative stress. Glia. 22, 371-378.

Kaptanoglu, E., Solaroglu, I., Okutan, O., Surucu, H.S., Akbiyik, F., Beskonakli, E. 2004. Erythropoietin exerts neuroprotection after acute spinal cord injury in rats: effect on lipid peroxidation and early ultrastructural findings. Neurosurg Rev. 27, 113-120.

Karadottir, R., Cavelier, P., Bergersen, L.H., Attwell, D. 2005. NMDA receptors are expressed in oligodendrocytes and activated in ischaemia. Nature. 438, 1162-1166.

Karim, Z., Sawada, A., Kawakami, H., Yamamoto, T., Taniguchi, T. 2006. A new calcium channel antagonist, lomerizine, alleviates secondary retinal ganglion cell death after optic nerve injury in the rat. Curr Eye Res. 31, 273-283.

Kennedy, C. (2007) Oxidised ATP. In: xPharm: The Comprehensive Pharmacology Reference(Editors-in-Chief: , S. J. E. and David, B. B., eds), pp 1-2 New York: Elsevier.

Khodorov, B. 2004. Glutamate-induced deregulation of calcium homeostasis and mitochondrial dysfunction in mammalian central neurones. Prog Biophys Mol Biol. 86, 279-351.

King, T.E., Barr, G.A. 2007. Spinal cord ionotropic glutamate receptors function in formalin-induced nociception in preweaning rats. Psychopharmacology (Berl). 192, 489-498.

Klein, K.U., Engelhard, K. 2010. Perioperative neuroprotection. Best Pract Res Clin Anaesthesiol. 24, 535-549.

Knoferle, J., Koch, J.C., Ostendorf, T., Michel, U., Planchamp, V., Vutova, P., Tonges, L., Stadelmann, C., Bruck, W., Bahr, M., Lingor, P. 2010. Mechanisms of acute axonal degeneration in the optic nerve in vivo. Proc Natl Acad Sci U S A. 107, 6064-6069.

Lasiene, J., Shupe, L., Perlmutter, S., Horner, P. 2008. No evidence for chronic demyelination in spared axons after spinal cord injury in a mouse. J Neurosci. 28, 3887-3896.

Lau, A., Tymianski, M. 2010. Glutamate receptors, neurotoxicity and neurodegeneration. Pflugers Arch. 460, 525-542.

Levkovitch-Verbin, H., Quigley, H.A., Martin, K.R., Zack, D.J., Pease, M.E., Valenta, D.F. 2003. A model to study differences between primary and secondary degeneration of retinal ganglion cells in rats by partial optic nerve transection. Invest Ophthalmol Vis Sci. 44, 3388-3393.

Li, S., Jiang, Q., Stys, P.K. 2000. Important role of reverse Na(+)-Ca(2+) exchange in spinal cord white matter injury at physiological temperature. J Neurophysiol. 84, 1116-1119.

Lobsiger, C.S., Cleveland, D.W. 2007. Glial cells as intrinsic components of non-cell-autonomous neurodegenerative disease. Nat Neurosci. 10, 1355-1360.

Matute, C. 1998. Characteristics of acute and chronic kainate excitotoxic damage to the optic nerve. Proc Natl Acad Sci U S A. 95, 10229-10234.

Matute, C., Torre, I., Perez-Cerda, F., Perez-Samartin, A., Alberdi, E., Etxebarria, E., Arranz, A.M., Ravid, R., Rodriguez-Antiguedad, A., Sanchez-Gomez, M., Domercq, M. 2007. P2X(7) receptor blockade prevents ATP excitotoxicity in oligodendrocytes and ameliorates experimental autoimmune encephalomyelitis. J Neurosci. 27, 9525-9533.

McTigue, D.M., Tripathi, R.B. 2008. The life, death, and replacement of oligodendrocytes in the adult CNS. J Neurochem. 107, 1-19.

Micu, I., Jiang, Q., Coderre, E., Ridsdale, A., Zhang, L., Woulfe, J., Yin, X., Trapp, B.D., McRory, J.E., Rehak, R., Zamponi, G.W., Wang, W., Stys, P.K. 2006.

NMDA receptors mediate calcium accumulation in myelin during chemical ischaemia. Nature. 439, 988-992.
Miller, R.H., Mi, S. 2007. Dissecting demyelination. Nat Neurosci. 10, 1351-1354.
Miller, R.J. 1991. The control of neuronal Ca2+ homeostasis. Progress in neurobiology. 37, 255-285.
Muir, K.W. 2006. Glutamate-based therapeutic approaches: clinical trials with NMDA antagonists. Curr Opin Pharmacol. 6, 53-60.
Nave, K.A. 2010. Myelination and the trophic support of long axons. Nat Rev Neurosci. 11, 275-283.
Norenberg, M.D., Smith, J., Marcillo, A. 2004. The pathology of human spinal cord injury: defining the problems. J Neurotrauma. 21, 429-440.
Paschen, W. 2001. Dependence of vital cell function on endoplasmic reticulum calcium levels: implications for the mechanisms underlying neuronal cell injury in different pathological states. Cell Calcium. 29, 1-11.
Payne, S.C., Bartlett, C.A., Harvey, A.R., Dunlop, S.A., Fitzgerald, M. 2011. Chronic swelling and abnormal myelination during secondary degeneration after partial injury to a central nervous system tract. J Neurotrauma. 28, 1077-1088.
Payne, S.C., Bartlett, C.A., Harvey, A.R., Dunlop, S.A., Fitzgerald, M. 2012. Myelin sheath decompaction, axon swelling, and functional loss during chronic secondary degeneration in rat optic nerve. Invest Ophthalmol Vis Sci. 53, 6093-6101.
Peng, T.I., Jou, M.J. 2010. Oxidative stress caused by mitochondrial calcium overload. Ann N Y Acad Sci. 1201, 183-188.
Petersen, M.S., Petersen, C.C., Agger, R., Hokland, M., Gundersen, H.J.G. 2006. A simple method for unbiased quantitation of adoptively transferred cells in solid tissues. Journal of Immunological Methods. 309, 173-181.
Phokeo, V., Kwiecien, J.M., Ball, A.K. 2002. Characterization of the optic nerve and retinal ganglion cell layer in the dysmyelinated adult Long Evans Shaker rat: evidence for axonal sprouting. J Comp Neurol. 451, 213-224.
Pitt, D., Gonzales, E., Cross, A.H., Goldberg, M.P. 2010. Dysmyelinated axons in shiverer mice are highly vulnerable to alpha-amino-3-hydroxy-5-methylisoxazole-4-propionic acid (AMPA) receptor-mediated toxicity. Brain Res. 1309, 146-154.
Rosenbluth, J. 2009. Multiple functions of the paranodal junction of myelinated nerve fibers. J Neurosci Res. 87, 3250-3258.
Saadoun, S., Papadopoulos, M.C. 2010. Aquaporin-4 in brain and spinal cord oedema. Neuroscience. 168, 1036-1046.
Saggu, S.K., Chotaliya, H.P., Blumbergs, P.C., Casson, R.J. 2010. Wallerian-like axonal degeneration in the optic nerve after excitotoxic retinal insult: an ultrastructural study. BMC Neurosci. 11, 97.
Salter, M.G., Fern, R. 2005. NMDA receptors are expressed in developing oligodendrocyte processes and mediate injury. Nature. 438, 1167-1171.
Selt, M., Bartlett, C.A., Harvey, A.R., Dunlop, S.A., Fitzgerald, M. 2010. Limited restoration of visual function after partial optic nerve injury; a time course study using the calcium channel blocker lomerizine. Brain Res Bull. 81, 467-471.
Stevens, B., Porta, S., Haak, L.L., Gallo, V., Fields, R.D. 2002. Adenosine: a neuron-glial transmitter promoting myelination in the CNS in response to action potentials. Neuron. 36, 855-868.

Sykova, E., Vargova, L. 2008. Extrasynaptic transmission and the diffusion parameters of the extracellular space. Neurochem Int. 52, 5-13.

Syntichaki, P., Tavernarakis, N. 2003. The biochemistry of neuronal necrosis: rogue biology? Nat Rev Neurosci. 4, 672-684.

Takahashi, M., Kohara, A., Shishikura, J., Kawasaki-Yatsugi, S., Ni, J.W., Yatsugi, S., Sakamoto, S., Okada, M., Shimizu-Sasamata, M., Yamaguchi, T. 2002. YM872: a selective, potent and highly water-soluble alpha-amino-3-hydroxy-5-methylisoxazole-4-propionic acid receptor antagonist. CNS Drug Rev. 8, 337-352.

Tamaki, Y., Araie, M., Fukaya, Y., Nagahara, M., Imamura, A., Honda, M., Obata, R., Tomita, K. 2003. Effects of lomerizine, a calcium channel antagonist, on retinal and optic nerve head circulation in rabbits and humans. Invest Ophthalmol Vis Sci. 44, 4864-4871.

Toriu, N., Akaike, A., Yasuyoshi, H., Zhang, S., Kashii, S., Honda, Y., Shimazawa, M., Hara, H. 2000. Lomerizine, a Ca2+ channel blocker, reduces glutamate-induced neurotoxicity and ischemia/reperfusion damage in rat retina. Exp Eye Res. 70, 475-484.

Wang, X., Arcuino, G., Takano, T., Lin, J., Peng, W.G., Wan, P., Li, P., Xu, Q., Liu, Q.S., Goldman, S.A., Nedergaard, M. 2004. P2X7 receptor inhibition improves recovery after spinal cord injury. Nat Med. 10, 821-827.

Weber, J.T. 2012. Altered calcium signaling following traumatic brain injury. Frontiers in Pharmacology. 3,

Wells, J., Kilburn, M.R., Shaw, J.A., Bartlett, C.A., Harvey, A.R., Dunlop, S.A., Fitzgerald, M. 2012. Early in vivo changes in calcium ions, oxidative stress markers, and ion channel immunoreactivity following partial injury to the optic nerve. J Neurosci Res. 90, 606-618.

Wong, E.H., Kemp, J.A. 1991. Sites for antagonism on the N-methyl-D-aspartate receptor channel complex. Annual review of pharmacology and toxicology. 31, 401-425.

Yamada, H., Chen, Y.N., Aihara, M., Araie, M. 2006. Neuroprotective effect of calcium channel blocker against retinal ganglion cell damage under hypoxia. Brain Res. 1071, 75-80.

Yanagisawa, K., Sato, S., O'Shannessy, D.J., Quarles, R.H., Suzuki, K., Miyatake, T. 1988. Myelin-associated calpain II. J Neurochem. 51, 803-807.

Figure Legends

Figure 1 Three Ca^{2+} channel inhibitors in combination preserved visual function. Mean ± SEM responses in the optokinetic nystagmus test of visual function; smooth pursuits (black) and fast resets (grey) / minute engaged in the task by control and treated animals 3 months after injury, Significant differences are indicated by * (compared to vehicle) or # (compared to normal) ($p \leq 0.05$).

Figure 2 Effects of combinations of Ca^{2+} channel inhibitors on neuronal somata and axons. Mean ± SEM βIII - tubulin+ RGC densities in ventral retina (A); mean ± SEM βIII - tubulin immunointensity in ventral ON (B) of control and treated animals 3 months after injury. Significant differences are indicated by * (compared to vehicle) or # (compared to normal) ($p \leq 0.05$) where observed.

Figure 3 Effects of combinations of Ca^{2+} channel inhibitors on ON swelling. Representative images of transverse sections of normal ON (A), at 3 months following partial transection (B) and an example of the various treatment groups (lomerizine, C), with quantification of cross-sectional ventral area for control and treated animals (D). Values were expressed as mean ± SEM, ventral area is expressed as μm^2. Significant differences are indicated by * (compared to vehicle) or # (compared to normal) ($p \leq 0.05$) where observed. Scale bars = 200 μm.

Figure 4 Effects of combinations of Ca^{2+} channel inhibitors on myelin decompaction. Representative images of axons ensheathed by myelin at varying stages of decompaction (A, arrows indicate decompaction, colour of arrow indicates degree of decompaction as detailed in the Figure legend), magnification is the same for all

images, scale bar = 1 μm. The distribution of axons with myelin of varying degrees of compaction is presented as a pie chart for: normal; injured and vehicle treated; or Lom / oxATP / INQ treated ventral ON at 3 months after injury (B). Quantification of the proportions of axons with normal myelin (C) or axons with partially decompacted myelin in ventral ON for control and treated animals (D); the proportions of axons (C, D) were expressed as a mean ± SEM (density of axons in axon type expressed as a proportion of total axon number counted in ventral ON). Significant differences are indicated by * (compared to vehicle) or # (compared to normal) ($p \leq 0.05$) where observed.

Figure 5 Effects of combinations of Ca^{2+} channel inhibitors on node / paranode complexes. The mean ± SEM length of the paranodal gap, indicative of node length, was quantified (μm; A) from control and treated animals 3 months after injury. Representative orthogonal projection of Caspr+ paranodes (green) and βIII - tubulin+ axons (red) demonstrates an atypical node / paranode complex (hemi - node, boxed) well within the z stack of collected images (B), scale bar = 5 μm. The mean ± SEM percentage of atypical node / paranode complexes (C), in normal and treated animals at 3 months was also quantified.

Figure 6 Effects of combinations of Ca^{2+} channel inhibitors on an oxidative stress indicator. Immunointensity of carboxymethyl lysine (CML, A) was quantified at 2 days after injury, in ventral ON, of control and treated animals. Significant differences are indicated by * (compared to vehicle) or # (compared to normal) ($p \leq 0.05$) where observed. (B) Representative images of co-localisation of CML (red) and olig1

(green) immunoreactivity (arrows) in normal, injured vehicle treated or Lom / oxATP / INQ treated ventral ON, 2 days following partial ON transection, scale bar = 25 μm.

Figure 1

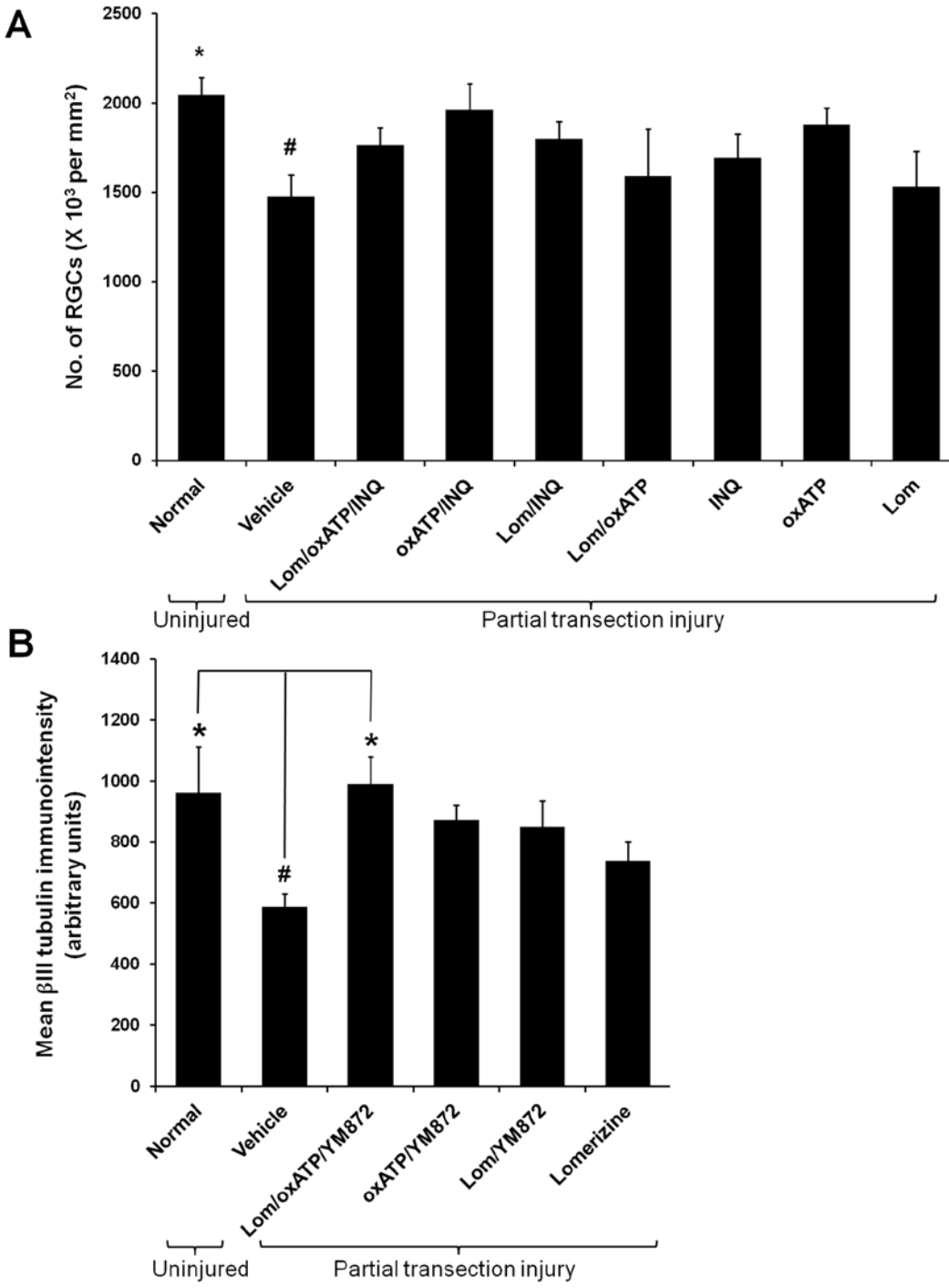
A
No. of RGCs (X 10³ per mm²)
2500
2000
1500
1000
500
0
*
#
Normal
Vehicle
Lom/oxATP/INQ
oxATP/INQ
Lom/INQ
Lom/oxATP
INQ
oxATP
Lom
Uninjured
Partial transection injury
B
Mean βIII tubulin immunointensity (arbitrary units)
1400
1200
1000
800
600
400
200
0
*
#
*
Normal
Vehicle
Lom/oxATP/YM872
oxATP/YM872
Lom/YM872
Lomerizine
Uninjured
Partial transection injury

Figure 2

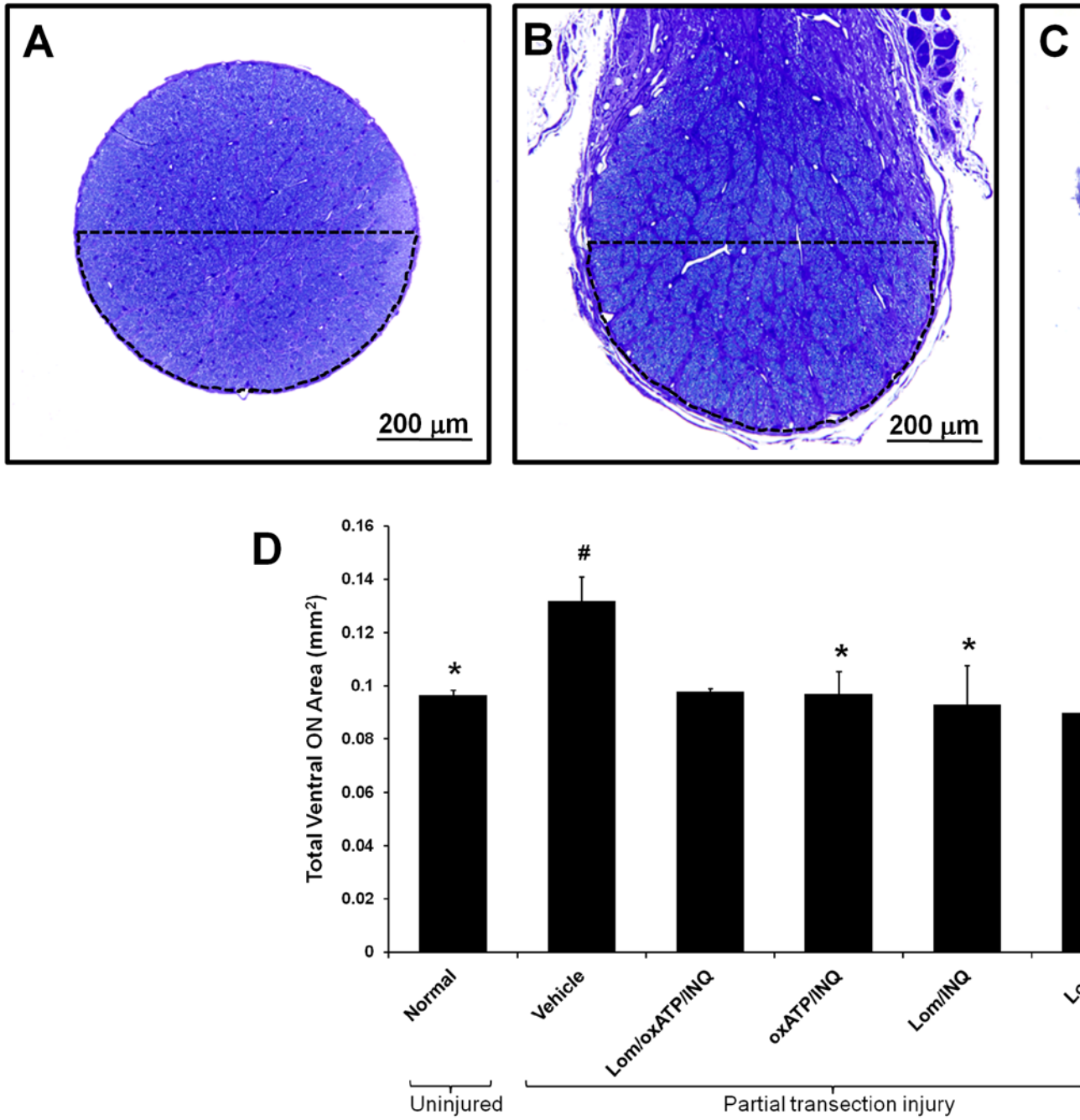
A
200 µm
B
200 µm
C
D
Total Ventral ON Area (mm²)
0.16
0.14
0.12
0.1
0.08
0.06
0.04
0.02
0
*
#
*
*
Normal
Vehicle
Lom/oxATP/INQ
oxATP/INQ
Lom/INQ
Uninjured
Partial transection injury

Figure 3

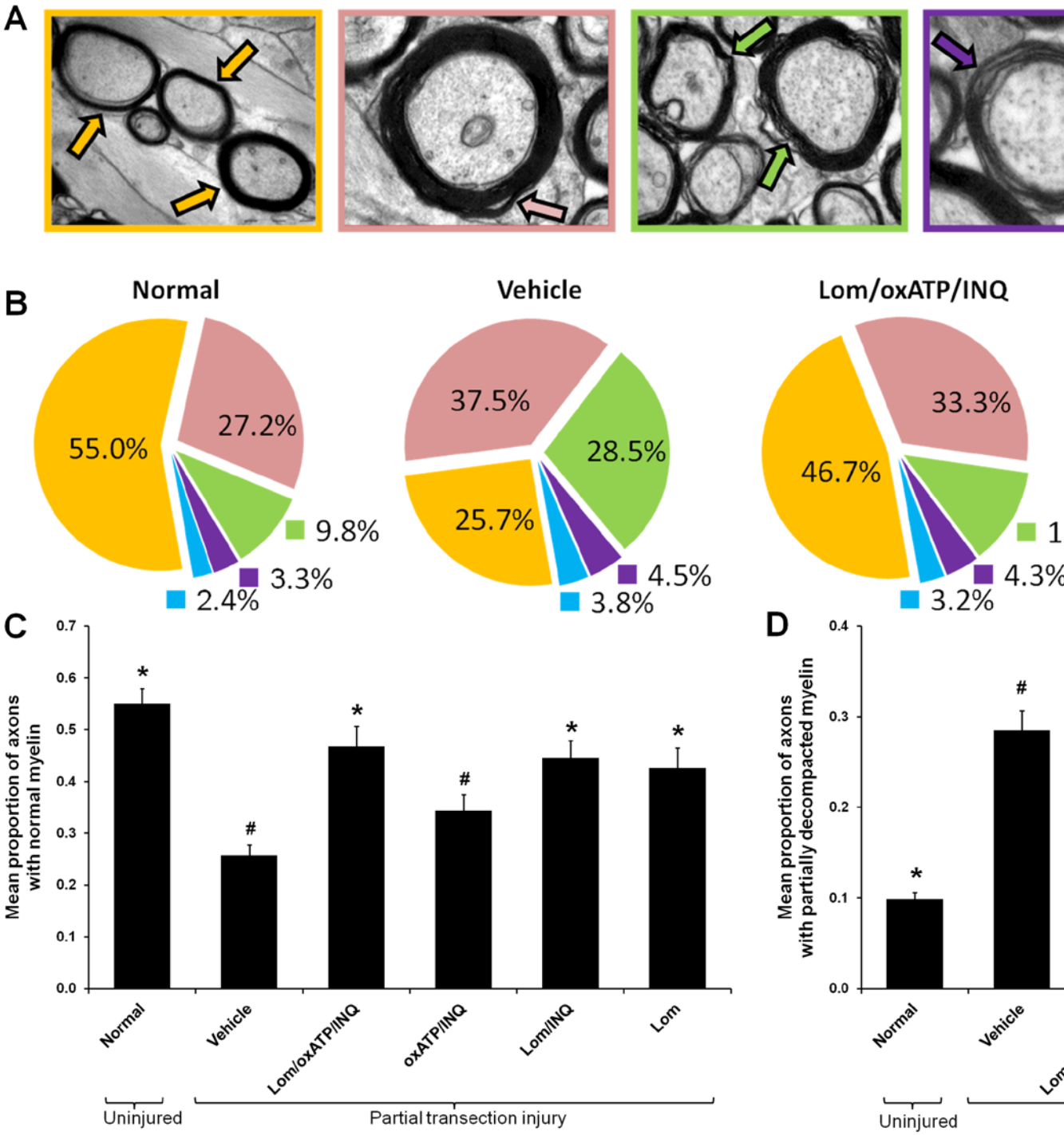
A
B
Normal
Vehicle
Lom/oxATP/INQ
55.0%
27.2%
9.8%
3.3%
2.4%
37.5%
28.5%
25.7%
4.5%
3.8%
33.3%
46.7%
4.3%
3.2%
C
Mean proportion of axons with normal myelin
0.0
0.1
0.2
0.3
0.4
0.5
0.6
0.7
Normal
Vehicle
Lom/oxATP/INQ
oxATP/INQ
Lom/INQ
Lom
Uninjured
Partial transection injury
D
Mean proportion of axons with partially decompacted myelin
0.0
0.1
0.2
0.3
0.4
Normal
Vehicle
Uninjured

Figure 4

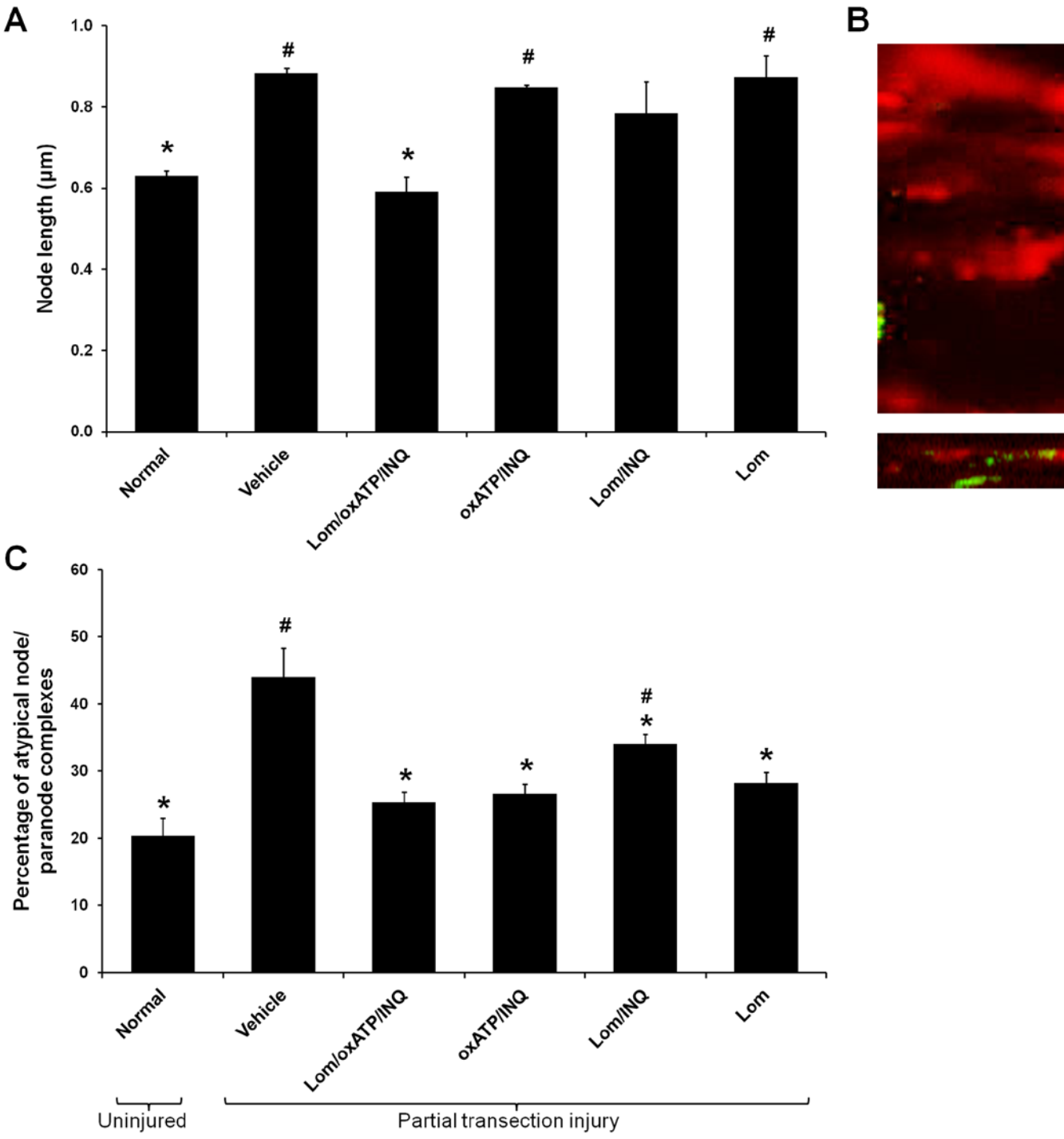
A
Node length (µm)
1.0
0.8
0.6
0.4
0.2
0.0
Normal
Vehicle
Lom/oxATP/INQ
oxATP/INQ
Lom/INQ
Lom
B
C
Percentage of atypical node/ paranode complexes
60
50
40
30
20
10
0
Uninjured
Partial transection injury

Figure 5

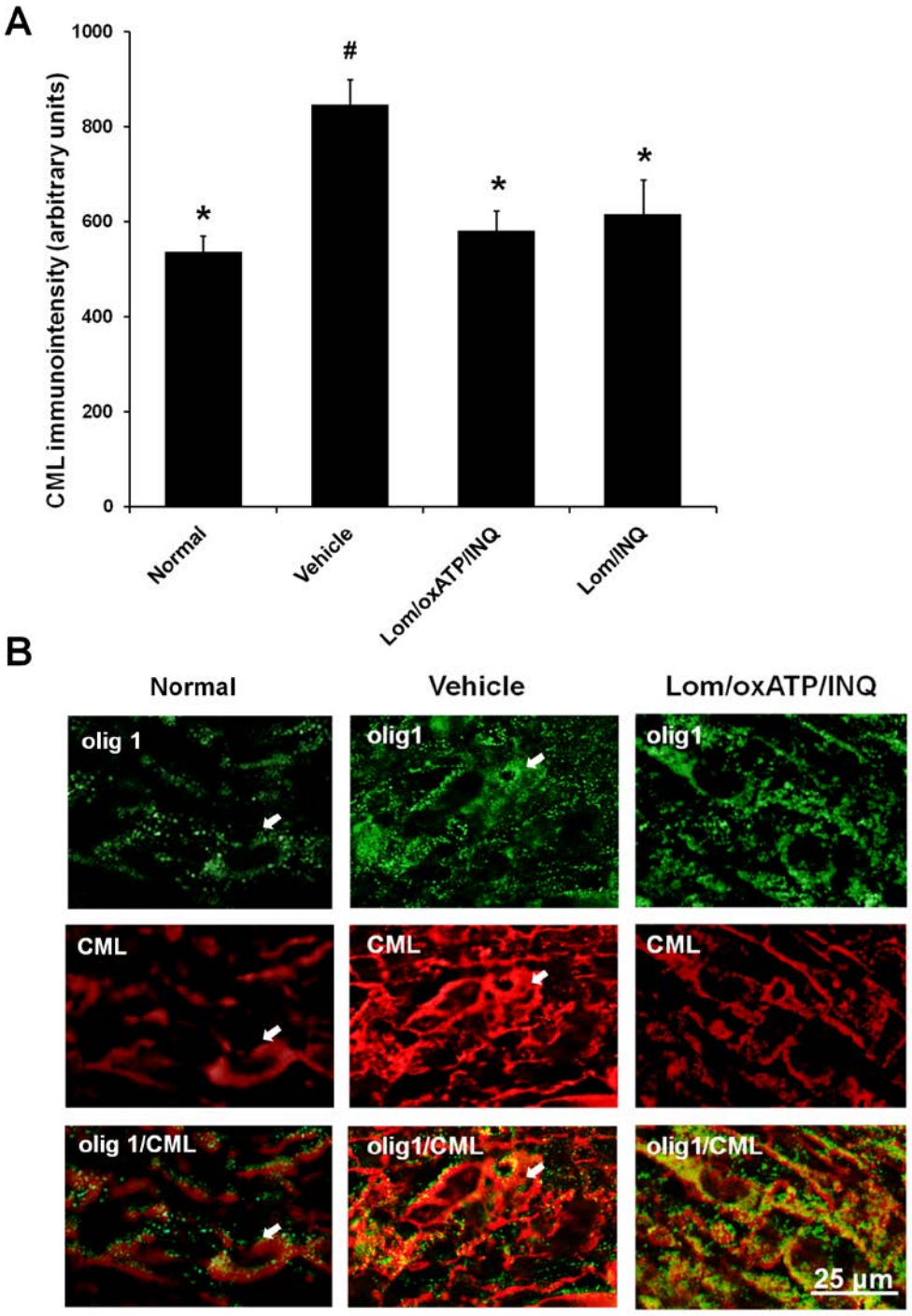
A
CML immunointensity (arbitrary units)
1000
800
600
400
200
0
#
*
*
*
Normal
Vehicle
Lom/oxATP/INQ
Lom/INQ
B
Normal
Vehicle
Lom/oxATP/INQ
olig 1
olig1
olig1
CML
CML
CML
olig 1/CML
olig1/CML
olig1/CML
25 µm

Figure 6

Table 1: Effects of combinations of Ca^{2+} channel inhibitors on secondary degeneration

Treatments/ **Outcomes**	***Vehicle***	***Lom/ oxATP/ INQ***	***oxATP/ INQ***	***Lom/ INQ***	***Lom/ oxATP***	***INQ***	***oxATP***	***Lom***
Visual function	↓	↑	ns	ns	ns	ns	ns	ns
RGC numbers	↓	ns	ns	ns	ns	ns	ns	ns
β-III tubulin IR	↓	↑	ns	ns	-	-	-	ns
ON ventral area	↑	ns	↓	↓	-	-	-	↓
Propn. axons with normal myelin	↓	↑	ns	↑	-	-	-	↑
Propn. axons with partially decompact myelin	↑	↓	~	↓	-	-	-	↓
Node length	↑	↓	↑	ns	-	-	-	↑
% Atypical complexes	↑	↓	↓	~	-	-	-	↓
Early oxidative stress	↑	↓	-	↓	-	-	-	-

Arrows ↑and↓ represent a statistically significant increase or decrease compared to normal vehicle) or to vehicle (for treatment groups) ($p \leq 0.05$); ns represents no significant differe compared to vehicle or normal; ~ represents an intermediate change, whereby the measu outcome was significantly different from both vehicle and / or normal. Visual function is numbe optokinetic nystagmus responses, IR is immunoreactivity, - is not done, Propn. is proportion